
BAYESIAN COMPOSITIONAL REGRESSION WITH FLEXIBLE MICROBIOME FEATURE AGGREGATION AND SELECTION

A PREPRINT

Satabdi Saha

Department of Biostatistics
The University of Texas MD Anderson Cancer Center,
Houston, TX
ssaha1@mdanderson.org

Liangliang Zhang

Department of Population and Quantitative Health Sciences
Case Western Reserve University
Cleveland, OH
lxz716@case.edu

Kim-Anh Do

Department of Biostatistics
The University of Texas MD Anderson Cancer Center,
Houston, TX
kimdo@mdanderson.org

Christine B. Peterson

Department of Biostatistics
The University of Texas MD Anderson Cancer Center,
Houston, TX
cbpeterson@mdanderson.org

June 4, 2024

ABSTRACT

Ongoing advances in microbiome profiling have allowed unprecedented insights into the molecular activities of microbial communities. This has fueled a strong scientific interest in understanding the critical role the microbiome plays in governing human health, by identifying microbial features associated with clinical outcomes of interest. Several aspects of microbiome data limit the applicability of existing variable selection approaches. In particular, microbiome data are high-dimensional, extremely sparse, and compositional. Importantly, many of the observed features, although categorized as different taxa, may play related functional roles. To address these challenges, we propose a novel compositional regression approach that leverages the data-adaptive clustering and variable selection properties of the spiked Dirichlet process to identify taxa that exhibit similar functional roles. Our proposed method, Bayesian Regression with Agglomerated Compositional Effects using a dirichLET process (BRACElet), enables the identification of a sparse set of features with shared impacts on the outcome, facilitating dimension reduction and model interpretation. We demonstrate that BRACElet outperforms existing approaches for microbiome variable selection through simulation studies and an application elucidating the impact of oral microbiome composition on insulin resistance.

1 Introduction

The microbiome, an incredibly diverse community of organisms, plays a pivotal role in human health and disease (Pflughoefl and Versalovic, 2012). Microbiome composition is highly heterogeneous, with notable diversity across individuals shaped by factors such as environment and dietary habits. Recent scientific studies have associated taxonomic or functional changes in the microbiome with a spectrum of health conditions. In particular, oral microbial abundances have been shown to correlate with systemic inflammation and insulin resistance (Demmer et al., 2017).

The methodological developments proposed in this work are motivated by the Oral Infections, Glucose Intolerance, and Insulin Resistance Study (ORIGINS) (Demmer et al., 2015), which seeks to characterize the association between the bacterial population of subgingival plaque and prediabetes. Oral microorganisms play a key role in shaping the risk of periodontal diseases, including periodontitis (Pihlstrom et al., 2005). It is postulated that chronic inflammation driven by the periodontal microbiota may contribute to impaired glucose regulation and heightened risk of insulin resistance, potentially laying the groundwork for type 2 diabetes (Gurav, 2012). Through our case study on the ORIGINS data, we aim to identify taxa associated with insulin resistance, shedding light on the influence of the periodontal microbiome on prediabetes.

In recent years, technological advancements have enabled direct quantification of microbiome composition. Most microbiome studies rely on sequencing of the 16S ribosomal RNA (rRNA) gene, which functions as a barcode that can be used to identify the bacterial species present in a sample. The analysis of microbiome profiling data poses numerous challenges (Peterson et al., 2024). First, due to limitations in sample collection and sequencing, the observed abundances can be interpreted only on a relative, rather than an absolute, scale. This characteristic renders the data inherently compositional and necessitates specialized analytical approaches (Gloor et al., 2017). Moreover, the high dimensionality of microbiome data necessitates sparse modeling techniques to identify relevant features for the prediction of clinical outcomes (Lin et al., 2014). Finally, microbiome data sets contain numerous rare features, for instance, those observed in less than 5% or 10% of subjects. Typically, these rare features are filtered out prior to downstream analysis (Callahan et al., 2016).

An alternative approach to filtering is to group features at higher taxonomic levels prior to predictive modeling. The observed features can be organized using taxonomic or phylogenetic trees. To obtain a taxonomic tree, the observed sequences are classified on the basis of their similarity to reference sequences for known organisms, generating a label that follows the traditional hierarchical classification *Kingdom, Phylum, Class, Order, Family, Genus, Species*. Phylogenetic trees, which can be obtained via bioinformatic pipelines, group features on the basis of their potential evolutionary relationships.

The challenge of linking the microbiome to human health outcomes can be framed as a regression problem with compositional predictors. In early work on compositional data analysis, Aitchison and Bacon-Shone (1984) proposed the linear log-contrast model for regression modeling with compositional covariates. Building on that idea, Lin et al. (2014) proposed applying an l_1 penalty to the coefficient vector of the linear log contrast model for sparse estimation of coefficients and improved prediction accuracy in the context of high-dimensional data. Shi et al. (2016) extended this work by selecting subcompositions of taxa at fixed taxonomic levels. Zhang et al. (2021) proposed a Bayesian model where the compositionality constraint was incorporated in the prior for the coefficient vector through a conditioning matrix with a controllable shrinkage parameter. To encourage joint selection of phylogenetically related features, the authors incorporated information from a known phylogenetic tree through an Ising prior. Zhang et al. (2024) proposed a Bayesian compositional generalized linear model that incorporates the phylogenetic relatedness among taxa through a structured regularized horseshoe prior. To deal with rare features, Bien et al. (2021) proposed grouping finer-resolution taxa into higher levels of taxonomic resolution by aggregating features over branches of a known tree and using the aggregated features in the outcome prediction.

However, these existing modeling approaches have critical limitations. The penalty-based methods proposed by Lin et al. (2014) and Shi et al. (2016) provide point estimates of regression coefficients that do not fully capture the uncertainty. In addition, these methods are optimized for prediction, rather than feature selection, and tend to have relatively high false positive rates (Zhang et al., 2021). The Bayesian approach proposed by Zhang et al. (2021) requires external information about a phylogenetic tree for estimation; this information reflects global genomic similarity between species, which may be an imperfect or noisy reflection of their functional similarity in driving an outcome of interest. Although Bien et al. (2021) account for the presence of rare features, they similarly rely on a fixed externally defined tree to achieve feature aggregation.

In this article, we introduce Bayesian Regression with Agglomerated Compositional Effects using a dirichLET process (BRACElet), a framework tailored for analyzing microbiome data that adeptly navigates inherent challenges such as its compositional structure, high dimensionality, and phylogenetic similarity. To effectively handle the fixed-sum constraint, we leverage current research in sampling from truncated multivariate normal densities. This method facilitates the direct

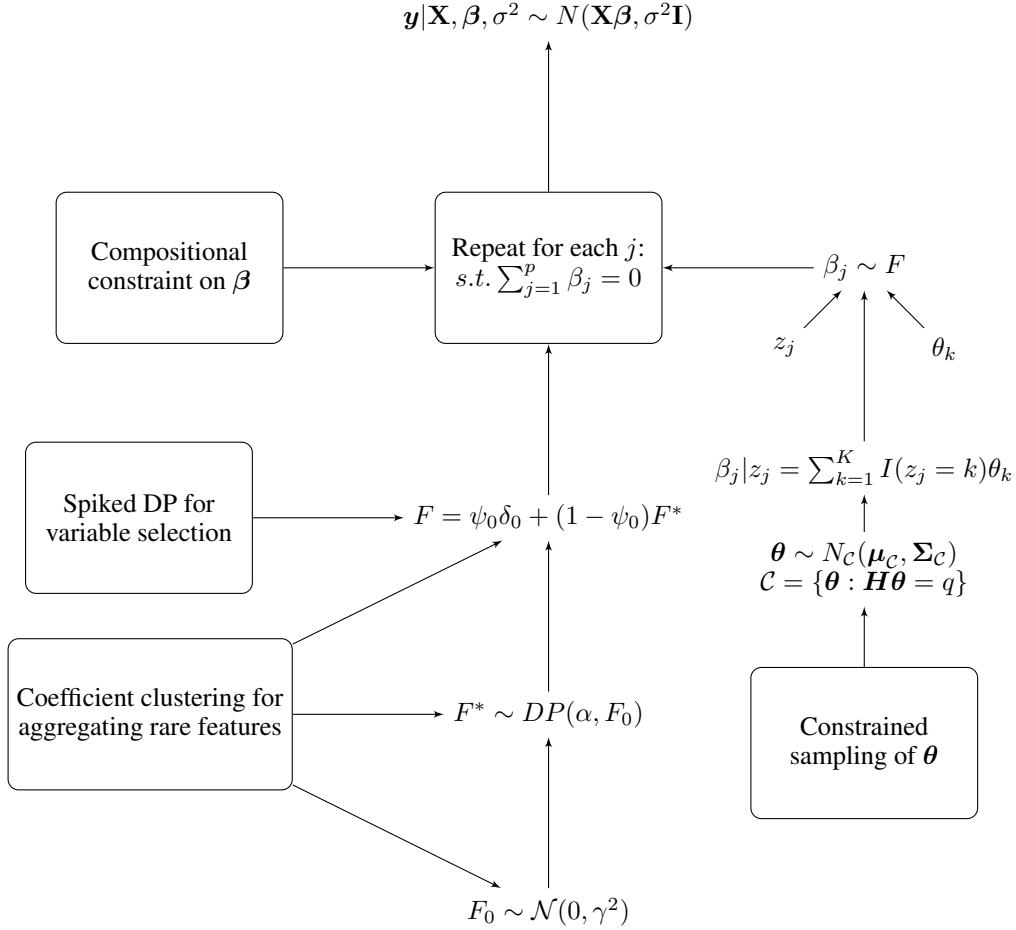


Figure 1: Overview figure for Bayesian compositional regression for high dimensional clustered effects

sampling of compositionally constrained regression coefficients within our Gibbs sampling framework. Additionally, we incorporate a spiked Dirichlet process prior to achieve sparse variable selection and allow for natural clustering of features in compositional microbiome profiles, thus effectively addressing the challenge posed by rare features. Through clustering the coefficients of sparsely observed features, we achieve substantial dimension reduction, resulting in denser features representing groups of organisms with shared effects, ultimately enhancing the prediction of clinical outcomes. Our innovative approach clusters regression coefficients in a data-adaptive manner, strategically collapsing rare features to generate denser groupings. To the best of our knowledge, BRACElet stands as the first Bayesian method for high-dimensional compositional regression with flexible microbiome feature aggregation and selection, avoiding a reliance on external taxonomic or phylogenetic tree information.

The remainder of the article is organized as follows: In Section 2, we provide a description of the proposed model and estimation procedure. In Section 3, we benchmark the performance of BRACElet against alternative approaches through simulation studies. In Section 4, we demonstrate the applicability of BRACElet through a study that aims to capture the relationship between subgingival microbial community composition and insulin resistance. Finally, Section 5 includes a discussion and concluding remarks.

2 Methods

2.1 Model specification

BRACElet builds on the compositional regression framework for the prediction of continuous outcomes from microbiome profiles. Let $\mathbf{y} = \{y_1, \dots, y_n\}$ denote the vector of continuous responses across n subjects, and \mathbf{U} denote the $n \times p$ observed microbial abundance matrix for p features. Notably, the sequencing methods used for generating the microbial abundances result in compositional data. Consequently, the observed counts are only interpretable on a relative scale, emphasizing their proportional rather than absolute nature. Prior to downstream analysis, the observed

abundance tables are generally converted to relative abundance matrices using a data transformation. To avoid numerical issues, the exact zeroes in the count matrix are generally replaced with a pseudocount of 0.5. To obtain the relative abundances, we rely on total sum scaling, where each element of the count matrix u_{ij} is divided by its sample sum $\sum_{j=1}^p u_{ij}$. The resulting relative abundance matrix $\tilde{\mathbf{U}}$ satisfies the compositional constraint $\sum_{j=1}^p \tilde{u}_{ij} = 1$. Each row of $\tilde{\mathbf{U}}$ is constrained to the simplex \mathcal{S}^p , rather than the unrestricted real space \mathbb{R}^p . $\tilde{\mathbf{U}}$ is then log transformed to obtain the log relative abundance matrix \mathbf{X} , where $\mathbf{X} = \log(\tilde{\mathbf{U}})$. Importantly, the p features in the matrix \mathbf{X} are still dependent due to the original compositionality constraint.

We now consider the formulation of the regression model relating the compositional microbiome data \mathbf{X} to the vector of clinical outcomes \mathbf{y} . To deal with compositional covariates, Aitchison and Bacon-Shone (1984) proposed the linear log-contrast model:

$$\mathbf{y} = \mathbf{C}_{\setminus p} \boldsymbol{\beta}_{\setminus p} + \boldsymbol{\varepsilon}, \quad (1)$$

where $\mathbf{C}_{\setminus p} = \log(u_{ij}/u_{ip})$ is an $n \times (p-1)$ matrix of the additive log-ratio transformed predictor variables, with the transformation done using the p^{th} predictor as the reference component, $\boldsymbol{\beta}_{\setminus p} = \{\beta_1, \dots, \beta_{p-1}\}$ is the vector of $p-1$ regression coefficients, and the entries in the noise vector are distributed independently as $\varepsilon_i \sim \mathcal{N}(0, \sigma^2)$, for $i = 1, \dots, n$. To eliminate the need to select a reference component, Lin et al. (2014) proposed solving an equivalent representation:

$$\mathbf{y} = \mathbf{X}\boldsymbol{\beta} + \boldsymbol{\varepsilon} \quad \text{subject to} \quad \sum_{j=1}^p \beta_j = 0. \quad (2)$$

The intercept term is omitted by centering the response and predictor variables. Lin et al. (2014) proposed imposing a penalty on the ℓ_1 norm of $\boldsymbol{\beta}$ to achieve sparsity. We innovate on this modeling framework by developing a novel Bayesian prior formulation that allows us to simultaneously handle the compositionality constraint, $\sum_{j=1}^p \beta_j = 0$; aggregate rare features; and achieve sparsity.

First, we discuss the idea of aggregating rare features. Given a known taxonomic or phylogenetic tree structure that captures the relatedness between features, a common strategy is to collapse or aggregate rare features and focus instead on internal nodes. A basic approach is to group finer-resolution taxa into higher levels of taxonomic resolution by summing over all the features that belong to the corresponding taxonomic classification. For example, it is quite common for microbiome data to be analyzed at the genus level, where the genus abundances are simply sums of the leaf node abundances for all leaf nodes assigned to the genus. More generally, suppose we obtain a new aggregated feature for the i th subject $x_{i,a} = x_{i,1} + x_{i,2} + \dots + x_{i,m}$, where m denotes the number of leaf nodes descending from the ancestor node a . As noted in Yan and Bien (2021), in the linear model setting, $x_{i,a}\boldsymbol{\beta} = (x_{i,1} + x_{i,2} + \dots + x_{i,m})\boldsymbol{\beta} = x_{i,1}\boldsymbol{\beta} + x_{i,2}\boldsymbol{\beta} + \dots + x_{i,m}\boldsymbol{\beta}$. Effectively, this means that learning a model where some features have exactly equal coefficients $\boldsymbol{\beta}$ corresponds to aggregation of the original rare features into a smaller set of more common features. The modeling objective then becomes estimation of the vector of coefficients such that rare features have common effects when supported by the data.

Instead of using a penalty function that enforces exact equality among coefficients on the basis of a known taxonomic tree structure, as in Bien et al. (2021), we propose to employ a Bayesian nonparametric prior on model coefficients. This strategy allows coefficients that cluster together to correspond to features that can be aggregated, providing flexibility in identifying sets of features with similar impacts on the outcome. Here, we build on the compositional regression model of equation (2). Rather than placing a classic spike-and-slab prior on each coefficient, we rely on a spiked Dirichlet process prior to both impose sparsity and allow clustering of the nonzero values.

We now provide the mathematical formulation of BRACElet. We place a spiked clustering prior on the coefficients β_j :

$$\begin{aligned} \beta_j | F &\sim F \quad \text{s.t.} \quad \sum_{j=1}^p \beta_j = 0, \\ F &\sim DP(\psi_0, \alpha, F_0). \end{aligned} \quad (3)$$

F is a spiked Dirichlet process (DP) prior (Dunson et al., 2008) that uses a mixture of a point mass at zero with a distribution given by a DP prior. The parameter ψ_0 is the prior probability of a coefficient being exactly zero, arising from a Dirac delta ‘‘spike’’ δ_0 . The DP prior is characterized by a concentration parameter α , a scalar controlling the degree of discretization, and a base distribution F_0 , i.e., $E(F) = F_0$. Mathematically, we can write the spiked DP as:

$$\begin{aligned} F &= \psi_0 \delta_0 + (1 - \psi_0) F^*, \\ F^* &\sim DP(\alpha, F_0), \\ F_0 &\sim N(0, \gamma^2). \end{aligned} \quad (4)$$

A key property of the Dirichlet process is that F is almost surely discrete, even if the base measure is continuous. In our setting, this means there will be ties among the β_j s corresponding to both exactly 0 and exactly shared coefficients in the regression model. In addition, the constraint on the β_j s accounts for the compositional structure of the covariates. This approach therefore induces a natural clustering of the coefficients, while allowing for sparsity in the presence of compositionality. Now, we provide a complete formulation of BRACElet’s hierarchical structure:

$$\begin{aligned} \mathbf{y}|\mathbf{X}, \boldsymbol{\beta}, \sigma^2 &\sim N(\mathbf{X}\boldsymbol{\beta}, \sigma^2\mathbf{I}) \\ \beta_j &\sim F \quad \text{s.t.} \quad \sum_{j=1}^p \beta_j = 0 \\ F &\sim DP(\psi_0, \alpha, F_0) \\ F &= \psi_0\delta_0 + (1 - \psi_0)F^* \\ F^* &\sim DP(\alpha, F_0) \\ F_0 &\sim \mathcal{N}(0, \gamma^2) \\ [\psi_0, (1 - \psi_0)] &\sim \text{Dirichlet}\left(\frac{\alpha_0}{2}, \frac{\alpha_0}{2}\right) \end{aligned}$$

To complete the model formulation, we place standard Inverse Gamma hyperpriors on the variance parameters, $\sigma^2 \sim IG(a_\sigma, b_\sigma)$ and $\gamma^2 \sim IG(a_\gamma, b_\gamma)$. This prior formulation allow for Gibbs updates of σ^2 and γ^2 from an Inverse Gamma. We place a non informative Gamma prior on the concentration parameter, $\alpha \sim \text{Gamma}(a_\alpha, b_\alpha)$, and update it using the method outlined in Escobar and West (1995). Finally, we set $\alpha_0 = 2$ which is equivalent to $\psi_0 \sim \text{Uniform}(0, 1)$.

To develop our computational approach, we leverage existing work on sampling for DP mixture models (Neal, 2000). To do so, we build on the stick-breaking construction (Sethuraman, 1994), a commonly utilized method for generating random samples from the DP process. In the stick-breaking view, a DP process F^* can be expressed as the infinite sum:

$$F^* = \sum_{k=1}^{\infty} \psi_k \delta_{\theta_k}, \quad (5)$$

where δ_{θ_k} is the indicator function that evaluates to zero everywhere except for $\delta_{\theta_k}(\theta_k) = 1$, $\psi_k = V_k \sum_{l=1}^{k-1} (1 - V_l)$, $V_k \sim \text{Beta}(1, \alpha)$, and $\theta_k \sim F_0$, for $k \geq 1$. Note that for the spiked DP process, we can write:

$$\begin{aligned} F &= \psi_0\delta_0 + (1 - \psi_0)F^* \\ &= \psi_0\delta_0 + (1 - \psi_0) \sum_{k=1}^{\infty} \psi_k \delta_{\theta_k} \\ &= \sum_{k=0}^{\infty} \tilde{\psi}_k \delta_{\theta_k}, \end{aligned} \quad (6)$$

where $\tilde{\psi}_0 = \psi_0$, $\tilde{\psi}_k = (1 - \psi_0)\psi_k$, and $\theta_0 = 0$. The spiked DP prior is therefore a special case of the DP prior, with the specific limitation that the first cluster equals zero. By modifying to the Gibbs sampler initially formulated by (Nott, 2008), we can accommodate this restriction and adapt the sampler for our purpose.

2.2 Posterior sampling

We now describe our approach for posterior sampling. Our novel algorithm addresses key technical challenges; in particular, we rely on recent advances in computational statistics to efficiently generate samples that satisfy the summation constraint on the model coefficients. More specifically, we leverage a new method for simulating hyperplane-truncated multivariate normal distributions. This advancement ensures that the regression estimates conform precisely to the p -dimensional simplex \mathcal{S}^p . In the remainder of this section, we provide an overview of our efficient Gibbs sampling approach, which enables feature selection and clustering while maintaining the compositional constraint on $\boldsymbol{\beta}$.

2.2.1 Steps of the Gibbs algorithm

Given a initial value for the set of regression coefficients $\boldsymbol{\beta} = (\beta_1, \dots, \beta_p)$, define $\boldsymbol{\theta} = (\theta_1, \dots, \theta_K)$ as the set of K ($K \leq p$) distinct elements of $\boldsymbol{\beta}$ (discreteness of the Dirichlet process may induce some repeated elements in $\boldsymbol{\beta}$), and the latent vector $\mathbf{z} = (z_1, \dots, z_p)$ such that $z_j = k$ if $\beta_j = \theta_k$. The model is reparametrized so that the latent vector \mathbf{z} gives the cluster labels of the regression coefficient vector $\boldsymbol{\beta}$, and $\boldsymbol{\theta}$ represents the set of cluster means. The reparametrized model is defined as:

$$f(\boldsymbol{\theta}, \mathbf{z}|\gamma^2, \alpha) = p(\mathbf{z}|\alpha)f(\boldsymbol{\theta}|\gamma^2, \mathbf{z}) \quad (7)$$

This prior structure follows directly from the Pólya urn representation of the Dirichlet process (Blackwell and MacQueen, 1973). The reparametrization plays a crucial role in MCMC sampling as it enables us to analytically integrate out the infinite-dimensional parameter F .

From the above formulation, it is clear that given \mathbf{z} , we need to estimate only K true effects $\boldsymbol{\theta}$. We define the $p \times K$ cluster membership matrix \mathbf{Z} such that $\mathbf{Z}_{jk} = 1$ if $z_j = k$, and 0 otherwise (Mehrotra and Maity, 2022). To update the cluster label z_j for predictor p , we need to calculate the posterior probability of the predictor p belonging to each cluster. We update \mathbf{z} to \mathbf{z}^* where

$$P(z_j = k | \mathbf{z}_{-j}, \gamma^2, \sigma^2, \alpha, \boldsymbol{\theta}, \mathbf{X}, \mathbf{y}) \propto P(z_j = k | \mathbf{z}_{-j}, \alpha) f(\mathbf{y} | \gamma^2, \sigma^2, \mathbf{X}, \mathbf{z}^*) \quad (8)$$

where

$$f(\mathbf{y} | \sigma^2, \gamma^2, \mathbf{z}, \mathbf{X}) = \int (2\pi\sigma^2)^{-n/2} \exp \left\{ \frac{-1}{2\sigma^2} (\mathbf{y} - \mathbf{X}_z \boldsymbol{\theta})^T (\mathbf{y} - \mathbf{X}_z \boldsymbol{\theta}) \right\} \times (2\pi\gamma^2)^{-K/2} \exp \left(-\frac{1}{2\gamma^2} \boldsymbol{\theta}^T \boldsymbol{\theta} \right) d\boldsymbol{\theta} \quad (9)$$

and \mathbf{z}^* is the vector of class labels with $z_j = k$ and $\mathbf{X}_z = \mathbf{XZ}^*$. Also,

$$P(z_j = k | \mathbf{z}_{-j}, \alpha) = \frac{m_{-j,k}}{p-1+\alpha}$$

$$P(z_j \neq z_l, \forall j \neq l | \mathbf{z}_{-j}, \alpha) = \frac{\alpha}{p-1+\alpha}, \quad (10)$$

where $m_{-j,k}$ is the number of $z_l, l \neq j$, that are equal to k . This formulation demonstrates that the conditional probability of an observation being assigned to an existing cluster is proportional to the number of elements in the cluster.

For the spiked DP model, the constraint for the zeroth cluster can be accounted for in equation (9) by dropping the columns in the zero cluster from \mathbf{X} , since their effects are restricted to be zero. If we define $p = p_0 + p_z$, where p_0 is the number of variables in the zeroth cluster and p_z is the number of elements in the nonzero clusters, then $\psi_0 = P(z_j = 0 | \mathbf{z}_{-j}, \alpha_0)$ can be sampled and the updates for \mathbf{z} can be modified as described in Neal (2000):

$$\psi_0 = P(z_j = 0 | \mathbf{z}_{-j}, \alpha_0) = \frac{m_{-j,0} + \alpha_0/2}{p-1+\alpha_0}$$

$$\text{For } K \geq 1, P(z_j = k | \mathbf{z}_{-j}, \alpha) = (1 - \psi_0) \frac{m_{-j,k}}{p_z - 1 + \alpha}$$

$$P(z_j \neq z_l, \forall j \neq l | \mathbf{z}_{-j}, \alpha) = (1 - \psi_0) \frac{\alpha}{p_z - 1 + \alpha} \quad (11)$$

We can then sample $\boldsymbol{\theta}$ from its posterior full conditional distribution, given $\mathbf{z}, \sigma^2, \gamma^2$, and α :

$$f(\boldsymbol{\theta} | \mathbf{z}, \sigma^2, \gamma^2, \alpha) \propto f(\boldsymbol{\theta} | \mathbf{z}, \gamma^2) f(\mathbf{y} | \boldsymbol{\theta}, \mathbf{z}, \sigma^2)$$

$$\propto \exp \left\{ -\frac{1}{2} \left(\boldsymbol{\theta}^T \boldsymbol{\Sigma}_\theta^{-1} \boldsymbol{\theta} - \frac{2}{\sigma^2} \mathbf{y}^T \mathbf{X}_z \boldsymbol{\theta} \right) \right\}, \quad (12)$$

which is a normal density with $\boldsymbol{\mu}_\theta = \boldsymbol{\Sigma}_\theta \frac{1}{\sigma^2} \mathbf{X}_z^T \mathbf{y}$ and $\boldsymbol{\Sigma}_\theta = \left(\frac{1}{\gamma^2} \mathbf{I} + \frac{1}{\sigma^2} \mathbf{X}_z^T \mathbf{X}_z \right)^{-1}$.

For each MCMC iteration, once we estimate the cluster labels \mathbf{z} and the set of unique regression coefficients $\boldsymbol{\theta}$, we can recover β_j using the formula $z_j = k$ if $\beta_j = \theta_k$. However, this sampling algorithm for $\boldsymbol{\beta}$ does not satisfy the compositionality constraint $\sum_{j=1}^p \beta_j = 0$ in Equation 3. In the following paragraph, we detail our modification of the sampling algorithm that allows for seamless integration of the compositionality constraint within the Gibbs sampling framework.

For the predictor variables, $j \in \{1, \dots, p\}$, $\beta_j | z_j = \sum_{k=1}^K I(z_j = k) \theta_k$, where K is the number of unique cluster labels in \mathbf{z} . This implies that $\beta_j \sim G = \sum_{k=0}^K \psi_k \delta_{\theta_k}(x)$ is a finite mixture of K delta functions at each step of the algorithm, which allows K to be infinite. For example, let $\boldsymbol{\theta} = \{\theta_1, \theta_2, \theta_3\}$ and $\mathbf{z} = \{1, 1, 1, 2, 2, 3\}$. Therefore, $\boldsymbol{\beta} = \{\theta_1, \theta_1, \theta_1, \theta_2, \theta_2, \theta_3\}$. In order to satisfy the compositionality constraint, we require that

$$\mathbf{1}^T \boldsymbol{\beta} = 0$$

$$\implies 3\theta_1 + 2\theta_2 + \theta_3 = 0$$

$$\implies \begin{pmatrix} 3 & 2 & 1 \end{pmatrix} \begin{pmatrix} \theta_1 \\ \theta_2 \\ \theta_3 \end{pmatrix} = 0$$

We can write this more generally as the following constraint on θ :

$$\mathbf{H}\theta = q.$$

Thus, we can sample θ from a truncated multivariate normal, where $\theta \sim N_{\mathcal{C}}(\mu_{\mathcal{C}}, \Sigma_{\mathcal{C}})$, over the constrained space $\mathcal{C} = \{\theta : \mathbf{H}\theta = q\}$. We leverage a sampling approach recently proposed by Cong et al. (2017) to efficiently simulate from this truncated multivariate normal distribution, utilizing $q = 0$ in our constraint. We incorporate the constrained sampling of θ within our Gibbs sampling setup and summarize the MCMC procedure for parameter estimation in Algorithm 1. The updates for γ^2 , σ^2 , and α can be done following the steps described in Nott (2008).

1. Update z by changing the group membership of each β_j
2. Sample θ given z , σ^2 , γ^2 , and α using equation (12): $\theta \sim N(\mu_{\theta}, \Sigma_{\theta})$
3. Set $\theta^* = \theta$. Input current state θ^*
4. Output $\theta = \theta^* + \Sigma_{\theta}\mathbf{H}^T(\mathbf{H}\Sigma_{\theta}\mathbf{H}^T)^{-1}(q - \mathbf{H}\theta^*)$
5. Use the compositionally constrained vector θ to proceed with the rest of the Gibbs sampling steps

Algorithm 1: Constrained sampling of θ subject to $\mathcal{S} = \{\theta : \mathbf{H}\theta = q\}$

3 Simulation studies

3.1 General setup

Our simulation setup is similar to the one described in Lin et al. (2014). We start by sampling an $n \times p$ data matrix \mathbf{U} from a multivariate normal distribution $N_p(\theta, \Sigma)$, and obtain the relative abundance matrix as $\mathbf{O} = \exp(\mathbf{U})/\mathbf{1}^T \exp(\mathbf{U})$. Using this transformation, the variables follow a logistic normal distribution (Aitchison and Shen, 1980), a commonly used distribution for modeling microbial abundances. In order to create microbiome features with varying abundance, we set $\theta_j = \log(0.5p)$ for $j = 1, \dots, 10$, and 0 otherwise, and we assume a covariance structure given by Σ . Finally, we generate the responses as $\mathbf{y} = \mathbf{X}\beta + \varepsilon$, where β is the vector of regression coefficients and $\mathbf{X} = \log(\mathbf{O})$. We consider settings with $n = 300$ and $p = 100, 300$, and 1000. We generate σ so that the signal-to-noise ratio (SNR) is 5, where $\text{SNR} = \text{mean}(|\beta_{\beta_j \neq 0}|/\sigma, j = 1, \dots, p)$. For each setting, we generate 100 simulated datasets, and randomly partition the data into training and test samples with a ratio of 80 : 20. The model is fitted on the training set, and the prediction error (PE) $= \frac{1}{n_{\text{test}}}(\mathbf{y}_{\text{test}} - \mathbf{X}_{\text{test}}\hat{\beta}_{\text{train}})^T(\mathbf{y}_{\text{test}} - \mathbf{X}_{\text{test}}\hat{\beta}_{\text{train}})$ and l_2 loss $\|\beta_{\text{true}} - \hat{\beta}_{\text{train}}\|_2$ are calculated on the test set. This process is repeated 100 times for each simulated dataset, and the mean and standard deviations of the results are reported.

We fit BRACElet to each simulated training data set using the Gibbs sampler described in Section 2.2, run for 10 000 iterations, with the first 5000 iterations used as burn-in. For all simulation settings, we use the following prior specification: $\gamma^2 \sim IG(0.001, 0.001)$, $\sigma^2 \sim IG(0.001, 0.001)$, $a_{\alpha} = 1/(0.75 \log p)^2$, and $b_{\alpha} = a_{\alpha}/\sqrt{p}$. This prior specification for α allows flexibility in the number of clusters. A detailed discussion on the choice of priors for α can be found in Escobar and West (1995) and Nott (2008).

3.2 Benchmarking methods

We compare the performance of BRACElet with that of the following existing approaches:

- lasso CLR: lasso regression (Tibshirani, 1996) on predictors transformed using the centered log ratio (CLR) transformation (Aitchison, 1986)
- lasso comp: penalized compositional regression approach proposed by Lin et al. (2014)
- BAZE: Bayesian variable selection for compositional data proposed by Zhang et al. (2021)
- BCGLM: Bayesian variable selection for generalized regression model with compositional predictors (Zhang et al., 2024)

The first approach considered, lasso CLR, relies on a data transformation to handle the compositionality of the predictors; the regression model itself does not account for compositionality. BAZE utilizes external information about the phylogenetic tree structure to guide the selection of important features, and imposes only mild shrinkage on selected

coefficients. BCGLM improves on BAZE by incorporating stronger shrinkage of the coefficients through a regularized horseshoe prior. However, since BCGLM employs continuous shrinkage, the estimates of the β coefficients are not exactly zero and some posterior thresholding mechanism needs to be applied for selection of the covariates. Finally, none of the benchmarking methods allows for coefficient clustering to account for rare features in the absence of a phylogenetic tree. We now describe the parameter settings we used for the benchmarking models. For the Bayesian models, we adopted the standard hyperpriors as recommended by the authors. In the case of BCGLM, results remained consistent when varying m_0 , the prior guess of the number of relevant predictors. Therefore, we set $m_0 = 10$. For BAZE, which relies on a phylogenetic tree-based similarity matrix \mathbf{Q} to capture the similarity between taxa, we set \mathbf{Q} to be a matrix consisting of zeroes to reflect a lack of prior information. For the frequentist approaches, lasso comp and lasso CLR, we used cross-validation to select the hyperparameters using the R package Compack.

To evaluate the variable selection performance of our proposed approach in settings with both independent and dependent compositional predictors, we design two simulation scenarios: one with independent covariates, and the other with varying levels of dependence among the covariates.

3.3 Setup 1: Independent covariates

For our first simulation setup, the nonzero elements of the vector β have three clusters of negative, zero, and positive values. The nonzero subvector of the true parameter vector β has 26 elements and is defined as $\beta_{nz} = \{\mathbf{1.5}_7, -\mathbf{1.75}_6\}$, where the numeric subscript indicates how many times the scalar value is repeated and $nz = \{(20+m) \cup (50+m)\}_{m=1}^{13}$. This vector satisfies the constraint that $\mathbf{1}^T \beta$ equals 0. To assume independence between the covariates, we set $\Sigma = \mathbf{I}$.

Table 1 displays the performance metrics, including prediction error, coefficient estimation accuracy, and number of false positives and false negatives, for continuous outcomes with true nonzero coefficients in the independent setup. BRACElet demonstrates superior performance compared to the Bayesian models BAZE and BCGLM in terms of test set prediction error. While lasso comp and lasso CLR show competitive out-of-sample prediction errors, they perform poorly in controlling false positives. Both BAZE and BRACElet exhibit excellent error rate control, with BCGLM closely following. All methods demonstrate perfect control over false negative errors. Particularly noteworthy is that the out-of-sample prediction error of BRACElet becomes more competitive as the number of predictors increases, underscoring its effectiveness in high-dimensional microbiome data regression.

Table 1: Performance comparison for simulated data with independent covariates, using sample size $n = 100$ and SNR = 5. Performance is summarized in terms of prediction error (PE), L2 loss in estimation of the coefficient vector, and number of false positives (FP) and false negatives (FN). Entries that reflect the smallest PE and L2 loss are marked in bold.

	Method	PE	L2 Loss	FP	FN
p = 100	lasso CLR	0.68 (0.07)	0.39 (0.07)	34.2 (6.72)	0.00 (0.00)
	lasso comp	0.67 (0.08)	0.39 (0.04)	33.7 (6.88)	0.00 (0.00)
	BAZE	0.68 (1.08)	0.23 (0.05)	0.00 (0.00)	0.00 (0.00)
	BCGLM	0.72 (0.10)	0.45 (0.04)	0.13 (0.42)	0.00 (0.00)
	BRACElet	0.56 (0.07)	0.14 (0.06)	0.00 (0.00)	0.00 (0.00)
p = 300	lasso CLR	0.68 (0.09)	0.50 (0.05)	63.7 (4.15)	0.00 (0.00)
	lasso comp	1.01 (0.16)	0.78 (0.09)	10.75 (3.77)	0.00 (0.00)
	BAZE	18.4 (22.9)	2.80 (3.19)	0.00 (0.00)	17.7 (10.9)
	BCGLM	0.51 (0.07)	0.59 (0.07)	0.20 (0.45)	0.00 (0.00)
	BRACElet	0.42 (0.03)	0.12 (0.06)	0.00 (0.10)	0.00 (0.00)
p = 1000	lasso CLR	0.91 (0.19)	0.69 (0.10)	120.5 (25.7)	0.00 (0.00)
	lasso comp	1.37 (0.36)	0.97 (0.15)	26.04 (7.18)	0.00 (0.00)
	BAZE	37.3 (32.6)	5.93 (3.28)	0.00 (0.00)	18.3 (10.3)
	BCGLM	0.52 (0.06)	0.32 (0.04)	0.08 (0.30)	0.00 (0.00)
	BRACElet	0.42 (0.02)	0.11 (0.05)	0.00 (0.10)	0.00 (0.00)

3.4 Dependent covariates

As correlations among microbiome features are common in practice, we consider two settings with dependent predictors. We introduce correlation in the data generation procedure by setting $\Sigma_{i,j} = \rho^{|i-j|}$ with $\rho = 0.2$ and 0.5. For both cases, we set the diagonal elements of Σ to 1. We construct a β vector with 35 nonzero elements across 9 clusters, with two clusters having only one element. The true parameter vector is given as $\beta = \{-\mathbf{0.8}_4, -\mathbf{1.41}_6, -\mathbf{1.95}_4, -1.16, 0.96, \mathbf{0}_3, \mathbf{1.04}_6, \mathbf{0.51}_4, \mathbf{1.95}_7, \mathbf{0}_{(p-37)}\}$. It is to be noted that β sums to 1 and its components have varying degrees of magnitude, implying varying strengths of association between the associated group of predictors and the response.

Table 2 displays the performance metrics, including prediction error, coefficient estimation accuracy, and number of false positives and false negatives, for the setting with $\rho = 0.2$. BRACElet outperforms the competing Bayesian models BAZE and BCGLM in terms of test set prediction error. BAZE closely follows in terms of out-of-sample prediction error and exhibits a slightly lower L2 loss in estimating the model coefficients. It is worth noting that BCGLM, implemented in STAN, is computationally intensive, requiring 10 hours to run a single replicate for $p = 1000$ in cases with $\rho = 0.2$ and $\rho = 0.5$. Therefore, the average results for BCGLM in these cases are based on only 10 random replicates instead of 100, and it shows the worst performance among all approaches. Among the frequentist methods, lasso CLR demonstrates competitive out-of-sample prediction error rates, but fails to effectively control the number of false positives for the higher-dimensional scenarios. BRACElet performs well in both the low and high-dimensional setups. As reported in Web Table 1 provided in the Supporting Information, the trends in the results remain consistent even when the dependence is increased to $\rho = 0.5$. Overall, BRACElet demonstrates great performance in terms of out-of-sample prediction error and false positive error control, outperforming the alternative methods in the majority of the simulation settings.

Since this simulation setting was the most challenging computationally, we considered it as a benchmark study for comparing the computational cost of the methods considered. We found that for the setting with $p = 100$, BCGLM required the longest run times (95 seconds for 1000 MCMC iterations), followed by BRACElet (78 seconds for 1000 MCMC iterations). The penalized methods and BAZE were more computationally efficient.

Table 2: Performance comparison for simulated data with dependent covariates using $\rho = 0.2$, sample size $n = 300$, and SNR = 5. Performance is summarized in terms of prediction error (PE), L2 loss in estimation of the coefficient vector, and number of false positives (FP) and false negatives (FN). Entries that reflect the smallest PE and L2 loss are marked in bold.

	Method	PE	L2 Loss	FP	FN
p = 100	lasso CLR	0.38 (0.08)	0.24 (0.02)	0.60 (0.78)	0.00 (0.00)
	lasso comp	0.11 (0.10)	0.08 (0.01)	27.2 (5.73)	0.00 (0.00)
	BAZE	0.13 (0.06)	0.06 (0.01)	0.00 (0.00)	0.00 (0.00)
	BCGLM	0.12 (0.02)	0.11 (0.01)	2.32 (1.67)	0.00 (0.00)
	BRACElet	0.10 (0.02)	0.08 (0.02)	0.00 (0.00)	0.00 (0.00)
p = 300	lasso CLR	0.41 (0.10)	0.26 (0.02)	1.47 (0.05)	0.00 (0.00)
	lasso comp	10.64 (3.34)	1.46 (0.18)	0.99 (1.00)	0.02 (0.15)
	BAZE	0.13 (0.09)	0.05 (0.01)	0.00 (0.00)	0.00 (0.00)
	BCGLM	0.20 (0.05)	0.34 (0.04)	2.40 (2.56)	0.00 (0.00)
	BRACElet	0.09 (0.01)	0.08 (0.02)	0.00 (0.00)	0.00 (0.00)
p = 1000	lasso CLR	0.48 (0.10)	0.28 (0.03)	7.72 (3.93)	0.00 (0.00)
	lasso comp	11.8 (3.36)	1.51 (0.19)	4.02 (2.54)	0.06 (0.24)
	BAZE	0.14 (0.03)	0.06 (0.01)	0.00 (0.00)	0.00 (0.00)
	BCGLM	49.1 (17.0)	3.25 (0.75)	0.00 (0.00)	12.5 (3.53)
	BRACElet	0.11 (0.02)	0.07 (0.02)	0.00 (0.00)	0.00 (0.00)

3.5 Dependent covariates with no clusters

Finally, to test whether BRACElet works in a setup with no clusters, we perform the simulation study described in Section 5.1 of Lin et al. (2014). We set $\theta_j = \log(0.5p)$ for $j = 1, \dots, 10$, and 0 otherwise, and set $\sigma = 0.5$. We include dependence by setting $\Sigma_{i,j} = \rho^{|i-j|}$ with $\rho = 0.5$. The true parameter vector is given as $\beta = \{1, -0.8, 0.6, 0, 0, -1.5, -0.5, 1.2, \dots, \mathbf{0}_{p-9}\}$. Table 3 displays the results for this simulation scenario with no clusters in the data. The performance of BRACElet is comparable to BCGLM and BAZE for $p = 100$ and 300. However, for $p = 1000$, the prediction error of BCGLM and BAZE are better than that of BRACElet. The competitive performance of BRACElet in this setting highlights its overall applicability, even in scenarios where there may be too many small clusters or no clusters at all. Importantly, if supporting prior information is available, we can also adjust the prior distribution of α to appropriately model such settings.

3.6 Clustering accuracy

In addition to variable selection and prediction, our proposed model facilitates the grouping of similar features through clustering of regression coefficients. In this subsection, we evaluate the clustering concordance between the true and predicted cluster labels. We obtain a single set of predicted labels from our MCMC samples using the SALS algorithm, which identifies the clustering that minimizes the posterior expected loss given a sequence of sampled labels (Dahl et al., 2022). As recommended by the authors of SALS, we use the generalized variation of information (VI) loss for

Table 3: Performance comparison for simulated data with no true clusters and dependent covariates using $\rho = 0.5$, sample size $n = 300$, and SNR = 5. Performance is summarized in terms of prediction error (PE), L2 loss in estimation of the coefficient vector, and number of false positives (FP) and false negatives (FN). Entries that reflect the smallest PE and L2 loss are marked in bold.

	Method	PE	L2 Loss	FP	FN
p = 100	lasso CLR	0.27 (0.02)	0.23 (0.05)	19.61 (7.71)	0.00 (0.00)
	lasso comp	0.27 (0.02)	0.22 (0.04)	21.73 (7.93)	0.00 (0.00)
	BAZE	0.30 (0.06)	0.09 (0.03)	0.05 (0.22)	0.00 (0.00)
	BCGLM	0.25 (0.02)	0.14 (0.03)	0.13 (0.42)	0.00 (0.00)
	BRACElet	0.24 (0.04)	0.12 (0.05)	0.03 (0.07)	0.00 (0.00)
p = 300	lasso CLR	0.31 (0.04)	0.32 (0.05)	34.0 (12.6)	0.00 (0.00)
	lasso comp	0.33 (0.05)	0.41 (0.07)	11.6 (5.27)	0.00 (0.00)
	BAZE	0.30 (0.05)	0.09 (0.03)	0.92 (0.95)	0.00 (0.00)
	BCGLM	0.27 (0.01)	0.15 (0.04)	0.13 (0.37)	0.00 (0.00)
	BRACElet	0.27 (0.04)	0.14 (0.05)	0.30 (0.19)	0.00 (0.00)
p = 1000	lasso CLR	0.34 (0.04)	0.41 (0.06)	52.31 (25.3)	0.00 (0.00)
	lasso comp	0.34 (0.04)	0.43 (0.05)	31.36 (8.79)	0.00 (0.00)
	BAZE	0.26 (0.02)	0.09 (0.03)	0.00 (0.00)	0.00 (0.00)
	BCGLM	0.26 (0.02)	0.14 (0.03)	0.06 (0.31)	0.00 (0.00)
	BRACElet	0.35 (0.06)	0.44 (0.08)	0.15 (0.85)	0.00 (0.00)

the optimization function. We compare the predicted cluster labels to the true cluster labels in the simulation setup using the adjusted Rand index (ARI), which has an expected value of 0 under a random assignment of labels and a value of 1 under perfect agreement. Given a set \mathbf{S} of n elements, and two clusterings of these elements, namely the true cluster labels $\mathbf{c} = \{c_1, \dots, c_{K_1}\}$ and predicted cluster labels $\mathbf{z} = \{z_1, \dots, z_{K_2}\}$, the overlap between \mathbf{c} and \mathbf{z} can be summarized in a contingency table $[n_{k_1 k_2}]$, where each entry $n_{k_1 k_2}$ denotes the number of objects in common between c_{k_1} and z_{k_2} : $n_{k_1 k_2} = |c_{k_1} \cap z_{k_2}|$. The adjusted Rand index is given as

$$ARI = \frac{\sum_{k_1 k_2} \binom{n_{k_1 k_2}}{2} - \left[\sum_{k_1} \binom{a_{k_1}}{2} \sum_{k_2} \binom{b_{k_2}}{2} \right] / \binom{n}{2}}{\frac{1}{2} \left[\sum_{k_1} \binom{a_{k_1}}{2} + \sum_{k_2} \binom{b_{k_2}}{2} \right] - \left[\sum_{k_1} \binom{a_{k_1}}{2} \sum_{k_2} \binom{b_{k_2}}{2} \right] / \binom{n}{2}}, \quad (13)$$

where n is the total number of objects being clustered, n_{ij} is the number of pairs of objects that belong to the same cluster in both the true and predicted clustering, a_{k_1} is the number of objects in the true cluster k_1 , and b_{k_2} is the number of objects in the predicted cluster k_2 . Figure 2 shows the clustering performance of our proposed method for the independent and dependent ($\rho = 0.2, 0.5$) simulation setup with the number of predictors set to $p = 100, 300$, and 1000. The clustering accuracy increases with an increase in the number of predictors as the size of the true null cluster increases and the model correctly predicts the clustering labels of the elements belonging to the null cluster. The ARI for the dependent cases is higher than for the independent case, and the performance is stable across the levels of dependence from 0.2 to 0.5. Overall, BRACElet achieves high values of the ARI for all cases, indicating its ability to recover the true cluster labels with high accuracy.

4 Application to oral microbiome data

To illustrate the utility of our proposed method, we applied it to data from the Oral Infections, Glucose Intolerance, and Insulin Resistance Study (ORIGINS), which investigated the correlation between periodontal microbiota and insulin resistance (Demmer et al., 2017). Previous studies have established a significant association between periodontitis, a chronic inflammatory disease affecting the tissues supporting the teeth, and the risk of type 2 diabetes. Type 2 diabetes, constituting 90% of diabetes cases, arises from disruptions in glucose regulation and insulin resistance. The cross-sectional ORIGINS study included 152 adults without diabetes (77% female), aged 20–55 years. The Human Oral Microbe Identification Microarray (Colombo et al., 2009) was used to quantify the abundance of 379 taxa in subgingival plaque samples. For this case study, we obtained the microbiome profiling data from Demmer et al. (2017). We utilized the observed insulin levels as our response variable, employing our proposed method to elucidate the relationship between the periodontal microbiome and insulin levels. We filtered the dataset to exclude samples lacking insulin level information and taxa with a total abundance lower than 30, resulting in 130 taxa and 111 samples. After filtering, there were no repeated measures (i.e., each sample corresponds to a unique subject). We replaced exact zeros in the count data with a small pseudocount of 0.5. We then transformed the counts into relative abundances and applied a log transformation to form the predictor matrix.

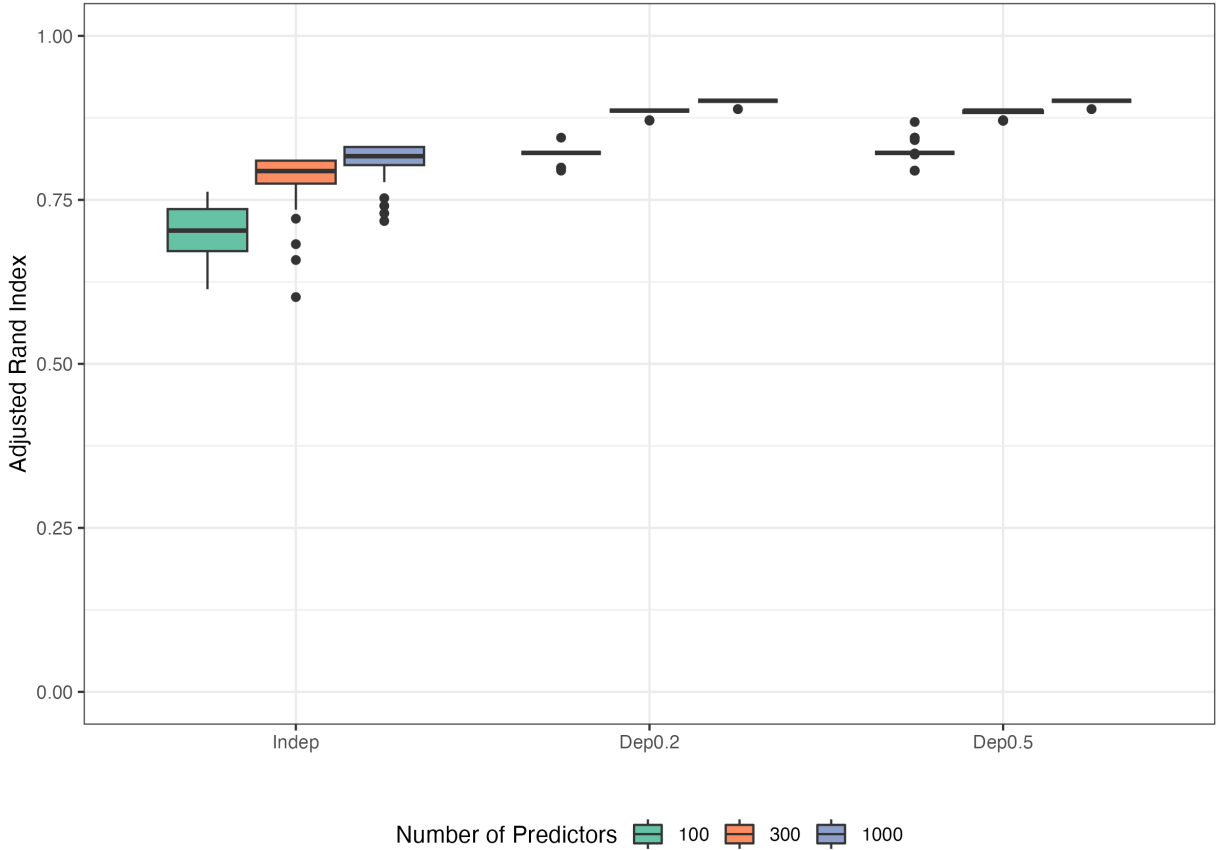


Figure 2: Boxplots showing the adjusted Rand indices calculated by comparing the true and predicted cluster labels in the independent and dependent ($\rho = 0.2, 0, 5$) setup with the number of predictors set to $p = 100, 300$, and 1000 .

4.1 Prediction and selection results

We randomly divided the 111 samples into a training set of 83 samples and a test set of 28 samples, and fit the proposed and benchmarking models on the training data. The process was repeated for 10 independent replicates, and we utilized these fitted models to calculate the prediction error on the test sets. The mean and standard deviation (in parentheses) of the prediction errors for the 10 replicates were 27.34 (9.63) for lasso CLR, 27.52 (9.67) for lasso comp, 25.38 (10.84) for BCGLM, and 24.70 (10.71) for BRACElet. This sample-splitting approach supports the utility of our proposed method in accurately identifying true patterns of microbiome association, and is consistent with our simulation results in that the proposed method achieves the lowest prediction error across the methods considered.

To gain further insights into the role of oral microbiome composition in regulating insulin levels, we fit the proposed model on the full data. To obtain a final clustering from the sampled cluster labels, we ran SALSO (Dahl et al., 2022) for a range of possible cluster numbers. As illustrated in Web Figure 1, the value of the expected VI loss decreased up to seven clusters, and plateaued after that. We therefore adopted seven clusters to achieve model parsimony. We obtained cluster means of -1.64, -0.85, -0.57, 0.05, 0.39, 1.29, and 1.49. Next, to achieve variable selection, we filtered out features that contained zero within their 95% posterior credible intervals. Based on these steps, BRACElet identified 38 features grouped into five nonzero clusters, as illustrated in Figure 3. It selected species belonging to the phyla Proteobacteria and Bacteroidota to be associated with insulin levels. At the genus level, BRACElet identified a number of species belong to *Prevotella*, *Tannerella*, and *Alloprevotella*.

We now discuss the findings in more detail, focusing on the bacterial species that confer increased risk. A cluster of nine species was identified as having the strongest positive association with increased insulin levels. Within this cluster, *Tannerella forsythia* had the largest effect size. *T. forsythia* has long been recognized as one of the bacteria that contribute to periodontitis (Socransky et al., 1998); more recently, increased abundance of *T. forsythia* in the oral microbiome has been associated with higher fasting blood glucose levels (Chang et al., 2023). This cluster also

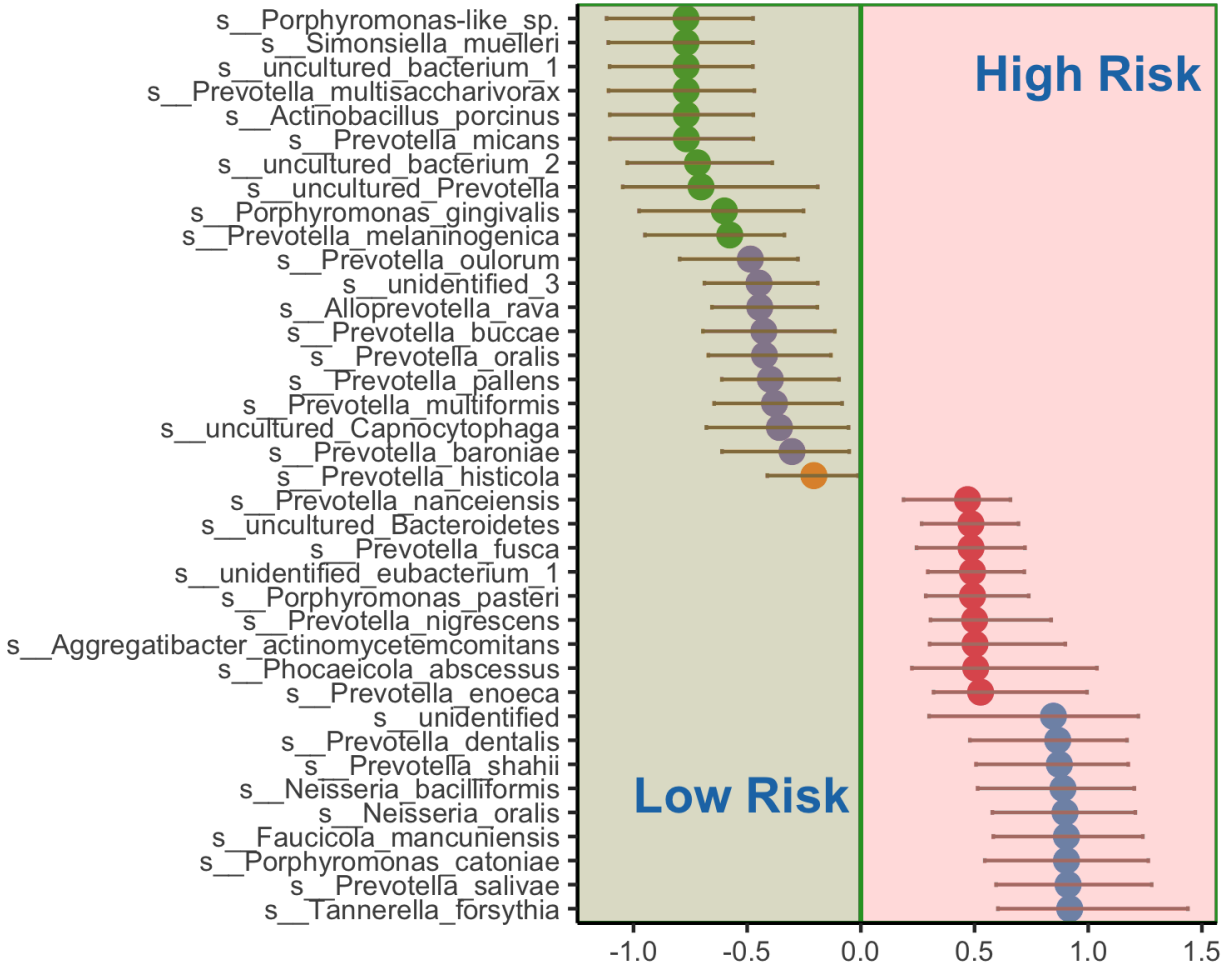


Figure 3: Parameter estimates and credible intervals for all features selected by BRACElet. The color of the dots determines the cluster labels of the estimates.

included three species belonging to the genus *Prevotella*, which supports the general understanding that *Prevotella* species contribute to increased inflammation (Könönen et al., 2022). However, our results do not unequivocally support this hypothesis, as we also identified several *Prevotella* species as having protective effects, reflecting heterogeneity across species within our dataset.

4.2 Concordance of cluster labels to phylogeny

We obtained a final clustering from the sampled cluster labels for our model using SALSO as described in Section 4.1. Our next goal was to investigate whether these taxa clusters demonstrate phylogenetic similarity. To achieve that goal, we first constructed a phylogenetic tree based on the representative sequences for the observed taxa. Next, we calculated the phylogenetic correlation matrix \mathbf{R} using the formula $r_{ij} = \frac{l_{ij}}{\sqrt{l_{ii}}\sqrt{l_{jj}}}$, where l_{aa} is defined as the branch length from the leaf node a to the root node, for $a = 1, \dots, p$, and l_{ij} is the shared branch length between leaf nodes i and j . This matrix was calculated using the R package *ape* (Paradis and Schliep, 2019) and is illustrated in Web Figure 2. We then applied hierarchical clustering on the correlation matrix to understand the overlap between our estimated cluster labels and a clustering based on phylogenetic similarity. Web Figure 3 demonstrates that there is a small degree of overlap between the BRACElet-determined cluster labels and the phylum-level groupings in the oral microbiome. This suggests that the groupings learned from BRACElet may offer additional insight on features with similar functional effects, and do not simply recapitulate known taxonomy.

Next, given the estimated cluster labels, we calculated the within-cluster and between-cluster mean phylogenetic correlations given in Figure 4, the hypothesis being that the within-cluster phylogenetic correlations will be higher

	1	2	3	4	5	6	7
1	0.3420	0.2861	0.2974	0.2888	0.2886	0.3059	0.3398
2	0.2861	0.3903	0.3740	0.3321	0.3518	0.3787	0.3376
3	0.2974	0.3740	0.4345	0.3655	0.4033	0.4337	0.3837
4	0.2888	0.3321	0.3655	0.3837	0.3713	0.3625	0.3416
5	0.2886	0.3518	0.4033	0.3713	0.4110	0.4138	0.3736
6	0.3059	0.3787	0.4337	0.3625	0.4138	0.4869	0.3961
7	0.3398	0.3376	0.3837	0.3416	0.3736	0.3961	0.4362

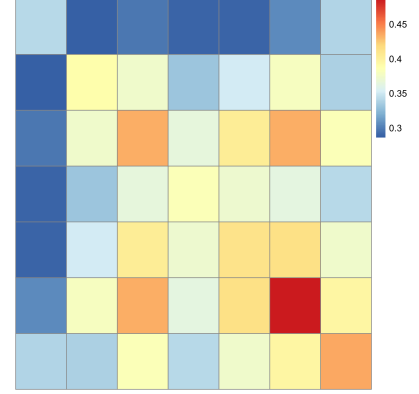


Figure 4: Table and heatmap showing the average phylogenetic correlations within and between the clusters for all features

than the between-cluster ones in most cases. The proportion of times the within-cluster correlations was greater than the between-cluster correlations, for all features, is 1.00, 1.00, 1.00, 1.00, 0.83, 1.00, 1.00. This result demonstrates that our model’s clustering scheme successfully captures some phylogenetic similarity between the taxa, without the need to prespecify this information as a model input. Taken together, we can conclude that the clusters identified by our proposed method have more phylogenetic similarity within clusters than across clusters, but reflect additional information on shared effects for a specific outcome.

5 Discussion

In this article, we present a novel statistical approach for microbiome compositional regression utilizing a nonparametric Bayesian approach for dimension reduction. Our proposed methodology represents a significant advancement in regression modeling of microbiome data for two key reasons. First, it introduces the inaugural application of Dirichlet process models for high-dimensional compositional regression with flexible microbiome feature aggregation and selection, circumventing the need for external phylogenetic information. Second, we develop a novel approach to address the compositional constraint in estimation of the regression coefficients. Through a combination of simulations and real data analysis, we illustrate the superior estimation and prediction performance of our proposed model compared to existing methods.

In our current work, we do not consider the presence of additional covariates, which could be relevant for many health-related studies. Our model can be easily extended to accommodate additional clinical or demographic variables by extending the model to $\mathbf{y} = \mathbf{X}\boldsymbol{\beta} + \mathbf{C}\boldsymbol{\zeta} + \boldsymbol{\varepsilon}$, where \mathbf{C} is the matrix of additional covariates and $\boldsymbol{\zeta}$, the vector of associated regression coefficients, has a normal prior distribution, $\boldsymbol{\zeta} \sim N(\mathbf{0}, \sigma_c^2 \mathbf{I})$. In addition, our formulation can be extended to model binary or count responses by changing the linear link function to probit/logit or log.

Finally, one of the main limitations of our work is the computational burden of inverting high-dimensional matrices while updating the cluster labels. The collapsed Gibbs sampler used in this paper is not scalable for high-dimensional cases if there is a large number of clusters in the data. Computational scalability can only be achieved when the number of clusters $k \ll p$, the number of predictors; therefore, we recommend that the Gibbs sampler be initialized with a small number of clusters. Faster methods that utilize approximation algorithms for DP priors, like variational Bayes approaches, have the potential to make our methodology more scalable for larger data sets with many clusters.

References

- Aitchison, J. (1986). *The Statistical Analysis of Compositional Data*. Chapman and Hall, London.
- Aitchison, J. and Bacon-Shone, J. (1984). Log contrast models for experiments with mixtures. *Biometrika*, 71(2):323–330.
- Aitchison, J. and Shen, S. M. (1980). Logistic-normal distributions: Some properties and uses. *Biometrika*, 67(2):261–272.
- Bien, J., Yan, X., Simpson, L., and Müller, C. L. (2021). Tree-aggregated predictive modeling of microbiome data. *Scientific Reports*, 11(1):14505.
- Blackwell, D. and MacQueen, J. B. (1973). Ferguson distributions via Pólya urn schemes. *The Annals of Statistics*, 1(2):353–355.

- Callahan, B. J., Sankaran, K., Fukuyama, J. A., McMurdie, P. J., and Holmes, S. P. (2016). Bioconductor workflow for microbiome data analysis: from raw reads to community analyses. *F1000Research*, 5.
- Chang, Y.-R., Cheng, W.-C., Hsiao, Y.-C., Su, G.-W., Lin, S.-J., et al. (2023). Links between oral microbiome and insulin resistance: Involvement of MAP kinase signaling pathway. *Biochimie*, 214:134–144.
- Colombo, A., Boches, S., Cotton, S., Goodson, J., Kent, R., et al. (2009). Comparisons of subgingival microbial profiles of refractory periodontitis, severe periodontitis, and periodontal health using the human oral microbe identification microarray. *Journal of Periodontology*, 80:1421–32.
- Cong, Y., Chen, B., and Zhou, M. (2017). Fast simulation of hyperplane-truncated multivariate normal distributions. *Bayesian Analysis*, 12(4):1017–1037.
- Dahl, D. B., Johnson, D. J., and Müller, P. (2022). Search algorithms and loss functions for Bayesian clustering. *Journal of Computational and Graphical Statistics*, 31(4):1189–1201.
- Demmer, R., Jacobs, D., Singh, R., Zuk, A., Rosenbaum, M., et al. (2015). Periodontal bacteria and prediabetes prevalence in ORIGINS: the oral infections, glucose intolerance, and insulin resistance study. *Journal of Dental Research*, 94(9_suppl):201S–211S.
- Demmer, R. T., Breskin, A., Rosenbaum, M., Zuk, A., LeDuc, C., et al. (2017). The subgingival microbiome, systemic inflammation and insulin resistance: The Oral Infections, Glucose Intolerance and Insulin Resistance Study. *Journal of Clinical Periodontology*, 44(3):255–265.
- Dunson, D. B., Herring, A. H., and Engel, S. M. (2008). Bayesian selection and clustering of polymorphisms in functionally related genes. *Journal of the American Statistical Association*, 103(482):534–546.
- Escobar, M. D. and West, M. (1995). Bayesian density estimation and inference using mixtures. *Journal of the American Statistical Association*, 90(430):577–588.
- Gloor, G. B., Macklaim, J. M., Pawlowsky-Glahn, V., and Egozcue, J. J. (2017). Microbiome datasets are compositional: and this is not optional. *Frontiers in Microbiology*, 8:2224.
- Gurav, A. N. (2012). Periodontitis and insulin resistance: casual or causal relationship? *Diabetes & Metabolism Journal*, 36(6):404.
- Könönen, E., Fteita, D., Gursoy, U. K., and Gursoy, M. (2022). *Prevotella* species as oral residents and infectious agents with potential impact on systemic conditions. *Journal of Oral Microbiology*, 14(1):2079814.
- Lin, W., Shi, P., Feng, R., and Li, H. (2014). Variable selection in regression with compositional covariates. *Biometrika*, 101(4):785–797.
- Mehrotra, S. and Maity, A. (2022). Simultaneous variable selection, clustering, and smoothing in function-on-scalar regression. *Canadian Journal of Statistics*, 50(1):180–199.
- Neal, R. M. (2000). Markov chain sampling methods for Dirichlet process mixture models. *Journal of Computational and Graphical Statistics*, 9(2):249–265.
- Nott, D. J. (2008). Predictive performance of Dirichlet process shrinkage methods in linear regression. *Computational Statistics & Data Analysis*, 52(7):3658–3669.
- Paradis, E. and Schliep, K. (2019). ape 5.0: an environment for modern phylogenetics and evolutionary analyses in R. *Bioinformatics*, 35:526–528.
- Peterson, C. B., Saha, S., and Do, K.-A. (2024). Analysis of microbiome data. *Annual Review of Statistics and Its Application*, 11:483–504.
- Pflughoeft, K. J. and Versalovic, J. (2012). Human microbiome in health and disease. *Annual Review of Pathology: Mechanisms of Disease*, 7:99–122.
- Pihlstrom, B. L., Michalowicz, B. S., and Johnson, N. W. (2005). Periodontal diseases. *The Lancet*, 366(9499):1809–1820.
- Sethuraman, J. (1994). A constructive definition of Dirichlet priors. *Statistica Sinica*, pages 639–650.
- Shi, P., Zhang, A., and Li, H. (2016). Regression analysis for microbiome compositional data. *Annals of Applied Statistics*, 10(2):1019–1040.
- Socransky, S., Haffajee, A., Cugini, M., Smith, C., and Kent Jr, R. (1998). Microbial complexes in subgingival plaque. *Journal of Clinical Periodontology*, 25(2):134–144.
- Tibshirani, R. (1996). Regression shrinkage and selection via the lasso. *Journal of the Royal Statistical Society Series B: Statistical Methodology*, 58(1):267–288.

-
- Yan, X. and Bien, J. (2021). Rare feature selection in high dimensions. *Journal of the American Statistical Association*, 116(534):887–900.
- Zhang, L., Shi, Y., Jenq, R. R., Do, K.-A., and Peterson, C. B. (2021). Bayesian compositional regression with structured priors for microbiome feature selection. *Biometrics*, 77(3):824–838.
- Zhang, L., Zhang, X., and Yi, N. (2024). Bayesian compositional generalized linear models for analyzing microbiome data. *Statistics in Medicine*, 43:141–155.